A FIXED POINT FRAMEWORK FOR RECOVERING SIGNALS FROM NONLINEAR TRANSFORMATIONS

1st Patrick L. Combettes
Department of Mathematics
North Carolina State University
Raleigh, NC 27695-8205, USA

2nd Zev C. Woodstock
Department of Mathematics
North Carolina State University
Raleigh, NC 27695-8205, USA

***Abstract*—We consider the problem of recovering a signal from nonlinear transformations, under convex constraints modeling *a priori* information. Standard feasibility and optimization methods are ill-suited to tackle this problem due to the nonlinearities. We show that, in many common applications, the transformation model can be associated with fixed point equations involving firmly nonexpansive operators. In turn, the recovery problem is reduced to a tractable common fixed point formulation, which is solved efficiently by a provably convergent, block-iterative algorithm. Applications to signal and image recovery are demonstrated. Inconsistent problems are also addressed.**

***Index Terms*—firmly nonexpansive operator, fixed point model, nonlinear transformation, signal recovery.**

I. Introduction

Under consideration is the general problem of recovering an original signal $\overline{x}$ in a Euclidean space $\mathcal{H}$ from a finite number of transformations $(r_k)_{k\in K}$ of the form

$$r_k = R_k\overline{x} \in \mathcal{G}_k, \tag{1}$$

where $R_k\colon \mathcal{H} \to \mathcal{G}_k$ is an operator mapping the solution space $\mathcal{H}$ to the Euclidean space $\mathcal{G}_k$. In addition to these transformations, some *a priori* constraints on $\overline{x}$ are available in the form of a finite family of closed convex subsets $(C_j)_{j\in J}$ of $\mathcal{H}$ [4], [14], [17], [18], [20]. Altogether, the recovery problem is to

$$\text{find } \ x \in \bigcap_{j\in J} C_j \ \text{ such that } \ (\forall k \in K) \quad R_k x = r_k. \tag{2}$$

One of the most classical instances of this formulation was proposed by Youla in [19], namely

$$\text{find } \ x \in V_1 \ \text{ such that } \ \text{proj}_{V_2} x = r_2, \tag{3}$$

where V_1 and V_2 are vector subspaces of $\mathcal{H}$ and proj_{V_2} is the projection operator onto V_2. As shown in [19], (3) covers many basic signal processing problems, such as band-limited extrapolation or image reconstruction from diffraction data, and it can be solved with a simple alternating projection algorithm. The extension of (3) to recovery problems with several transformations modeled as linear projections $r_k = \text{proj}_{V_k}\overline{x}$ is discussed in [9], [13]. More broadly, if the operators $(R_k)_{k\in K}$ are linear, reliable algorithms are available to solve (2). In particular, since the associated constraint set is an affine subspace with an explicit projection operator, standard feasibility algorithms can be used [4]. Alternatively, proximal splitting methods can be considered; see [6] and its references.

In the present paper we consider the general situation in which the operators $(R_k)_{k\in K}$ in (1) are not necessarily linear, a stark departure from common assumptions in signal recovery problems. Examples of such nonlinearly generated data $(r_k)_{k\in K}$ in (1) include hard-thresholded wavelet coefficients of $\overline{x}$, the positive part of the Fourier transform of $\overline{x}$, a mixture of best approximations of $\overline{x}$ from closed convex sets, a maximum a posteriori denoised version of $\overline{x}$, or measurements of $\overline{x}$ acquired through nonlinear sensors.

A significant difficulty one faces in the nonlinear context is that the constraint (1) is typically not representable by an exploitable convex constraint; see, e.g., [2], [3]. As a result, finding a solution to (2) with a provenly convergent and numerically efficient algorithm is a challenging task. In particular, standard convex feasibility algorithms are not applicable. Furthermore, variational relaxations involving a penalty of the type $\sum_{k\in K}\phi_k(\|R_k x - r_k\|)$ typically lead to nonconvex problems, even for choices as basic as $\phi_k = |\cdot|^2$ and R_k taken as the projection operator onto a closed convex set.

Our strategy to solve (2) is to forego the feasibility and optimization approaches in favor of the flexible and unifying framework of fixed point theory. Our first contribution is to show that, while R_k in (1) may be a very badly conditioned (possibly discontinuous) operator, common transformation models can be reformulated as fixed point equations with respect to an operator with much better properties, namely a firmly nonexpansive operator. Next, using a suitable modeling of the constraint sets

The work of P. L. Combettes was supported by the National Science Foundation under grant CCF-1715671 and the work of Z. C. Woodstock was supported by the National Science Foundation under grant DGE-1746939.

$(C_j)_{j\in J}$, we rephrase (2) as an equivalent common fixed point problem and solve it with a reliable and efficient extrapolated block-iterative fixed point algorithm. This strategy is outlined in Section II, where we also provide the algorithm. In Section III, we present several numerical illustrations of the proposed framework to nonlinear signal and image recovery. Finally, inconsistent problems are addressed in Section IV.

II. Fixed point model and algorithm

For background on the tools from fixed point theory and convex analysis used in this section, we refer the reader to [1]. Let us first recall that an operator $T\colon \mathcal{H}\to\mathcal{H}$ is firmly nonexpansive if

$$(\forall x\in\mathcal{H})(\forall y\in\mathcal{H})\quad \|Tx-Ty\|^2\leqslant \|x-y\|^2-\|(\mathrm{Id}\,-T)x-(\mathrm{Id}\,-T)y\|^2, \quad (4)$$

and firmly quasinonexpansive if

$$(\forall x\in\mathcal{H})(\forall y\in \operatorname{Fix}T)\quad \langle y-Tx\mid x-Tx\rangle\leqslant 0, \quad (5)$$

where $\operatorname{Fix}T=\big\{x\in\mathcal{H}\;\big|\;Tx=x\big\}$. Finally, the subdifferential of a convex function $f\colon\mathcal{H}\to\mathbb{R}$ at $x\in\mathcal{H}$ is

$$\partial f(x)=\big\{u\in\mathcal{H}\big|(\forall y\in\mathcal{H})\,\langle y-x\mid u\rangle+f(x)\leqslant f(y)\big\}. \quad (6)$$

As discussed in Section I, the transformation model (1) is too general to make finding a solution to (2) via a provenly convergent method possible. We therefore assume the following.

Assumption 1 The problem (2) has at least one solution, $J\cap K=\varnothing$, and the following hold:

(i) For every $k\in K$, R_k is *proximinal*: there exists $S_k\colon\mathcal{G}_k\to\mathcal{H}$ such that $S_k\circ R_k$ is firmly nonexpansive and $(\forall x\in\bigcap_{j\in J}C_j)\;S_k(R_kx)=S_kr_k\Rightarrow R_kx=r_k$.

(ii) For every $j\in J_1\subset J$, the operator $\operatorname{proj}_{C_j}$ is easily implementable.

(iii) For every $j\in J\smallsetminus J_1$, $f_j\colon\mathcal{H}\to\mathbb{R}$ is a convex function such that $C_j=\big\{x\in\mathcal{H}\;\big|\;f_j(x)\leqslant 0\big\}$.

In view of Assumption 1(i), let us replace (2) by the equivalent problem

$$\text{find } x\in\bigcap_{j\in J}C_j \text{ such that } (\forall k\in K)\;S_k(R_kx)=S_kr_k. \quad (7)$$

Concrete examples of suitable operators $(S_k)_{k\in K}$ will be given in Section III (see also [10]). The motivation behind (7) is that it leads to a tractable fixed point formulation. To see this, set

$$(\forall k\in K)\quad T_k=S_kr_k+\mathrm{Id}\,-S_k\circ R_k \quad (8)$$

and let $x\in\bigcap_{j\in J}C_j$. Then, for every $k\in K$, (1) $\Leftrightarrow$ $S_k(R_kx)=S_kr_k\Leftrightarrow x=S_kr_k+x-S_k(R_kx)\Leftrightarrow x\in\operatorname{Fix}T_k$. A key observation at this point is that (4) implies that the operators $(T_k)_{k\in K}$ are firmly nonexpansive, hence firmly quasinonexpansive.

If $j\in J_1$, per Assumption 1(ii), the set C_j will be activated in the algorithm through the use of the operator $T_j=\operatorname{proj}_{C_j}$, which is firmly nonexpansive [1, Proposition 4.16]. On the other hand, if $j\in J\smallsetminus J_1$, the convex inequality representation of Assumption 1(iii) will lead to an activation of C_j through its subgradient projector. Recall that the subgradient projection of $x\in\mathcal{H}$ onto C_j relative to $u_j\in\partial f_j(x)$ is

$$T_jx=\begin{cases}x-\dfrac{f_j(x)}{\|u_j\|^2}u_j, & \text{if } f_j(x)>0;\\ x, & \text{if } f_j(x)\leqslant 0,\end{cases} \quad (9)$$

and that T_j is firmly quasinonexpansive, with $\operatorname{Fix}T_j=C_j$ [1, Proposition 29.41]. The advantage of the subgradient projector onto C_j is that, unlike the exact projector, it does not require solving a nonlinear best approximation problem, which makes it much easier to implement in the presence of convex inequality constraints [5]. Altogether, (2) is equivalent to the common fixed point problem

$$\text{find } x\in\bigcap_{i\in J\cup K}\operatorname{Fix}T_i, \quad (10)$$

where each T_i is firmly quasinonexpansive. This allows us to solve (2) as follows.

Theorem 2 [10] *Consider the setting of problem* (2) *under Assumption 1. Let $x_0\in\mathcal{H}$, let $0<\varepsilon<1/\operatorname{card}(J\cup K)$, and set $(\forall k\in K)\;p_k=S_kr_k$ and $F_k=S_k\circ R_k$. Iterate*

$$\begin{array}{l}
\textit{for } n=0,1,\ldots\\
\quad\varnothing\neq I_n\subset J\cup K\\
\quad\{\omega_{i,n}\}_{i\in I_n}\subset[\varepsilon,1],\ \textstyle\sum_{i\in I_n}\omega_{i,n}=1\\
\quad\textit{for every } i\in I_n\\
\quad\quad\textit{if } i\in J_1\\
\quad\quad\quad y_{i,n}=\operatorname{proj}_{C_i}x_n-x_n\\
\quad\quad\textit{if } i\in J\smallsetminus J_1\\
\quad\quad\quad u_{i,n}\in\partial f_i(x_n)\\
\quad\quad\quad y_{i,n}=\begin{cases}-\dfrac{f_i(x_n)}{\|u_{i,n}\|^2}u_{i,n} & \textit{if } f_i(x_n)>0\\ 0, & \textit{if } f_i(x_n)\leqslant 0\end{cases}\\
\quad\quad\textit{else}\\
\quad\quad\quad y_{i,n}=p_i-F_ix_n\\
\quad\quad\nu_{i,n}=\|y_{i,n}\|\\
\quad\nu_n=\textstyle\sum_{i\in I_n}\omega_{i,n}\nu_{i,n}^2\\
\quad\textit{if } \nu_n=0\\
\quad\quad x_{n+1}=x_n\\
\quad\textit{else}\\
\quad\quad y_n=\textstyle\sum_{i\in I_n}\omega_{i,n}y_{i,n}\\
\quad\quad\Lambda_n=\nu_n/\|y_n\|^2\\
\quad\quad\lambda_n\in[\varepsilon,(2-\varepsilon)\Lambda_n]\\
\quad\quad x_{n+1}=x_n+\lambda_ny_n.
\end{array} \quad (11)$$

Suppose that there exists an integer $M>0$ such that

$$(\forall n\in\mathbb{N})\quad \bigcup_{m=0}^{M-1}I_{n+m}=J\cup K. \quad (12)$$

Then $(x_n)_{n\in\mathbb{N}}$ *converges to a solution to* (2).

When $K = \varnothing$, (11) coincides with the extrapolated method of parallel subgradient projections (EMOPSP) of [5]. It has in addition the ability to incorporate the constraints (1), while maintaining the attractive features of EMOPSP. First, it can process the operators in blocks of variable size. The control scheme (12) just imposes that every operator be activated at least once within any M consecutive iterations. Second, because the extrapolation parameters $(\Lambda_n)_{n\in\mathbb{N}}$ can attain large values in $[1, +\infty[$, large steps are possible, which lead to fast convergence compared to standard relaxation schemes, where $\Lambda_n \equiv 1$.

III. Applications

We illustrate several instances of (2), develop tractable reformulations of the form (7), and solve them using (11), where $x_0 = 0$ and the relaxation strategy is that recommended in [4, Chapter 5], namely

$$(\forall n \in \mathbb{N}) \quad \lambda_n = \begin{cases} \Lambda_n/2, & \text{if } n = 0 \mod 3; \\ 1.99\Lambda_n, & \text{otherwise.} \end{cases} \tag{13}$$

A. Restoration from distorted signals

The goal is to recover the original form of the N-point ($N = 2048$) signal $\overline{x}$ from the following (see Fig. 1):

- A bound γ_1 on the energy of the finite differences of $\overline{x}$, namely $\|D\overline{x}\| \leqslant \gamma_1$, where $D\colon (\xi_i)_{i\in\{0,\dots,N-1\}} \mapsto (\xi_{i+1} - \xi_i)_{i\in\{0,\dots,N-2\}}$. The bound is given from prior information as $\gamma_1 = 1.17$.
- A distortion $r_2 = R_2\overline{x}$, where R_2 clips componentwise to $[-\gamma_2, \gamma_2]$ ($\gamma_2 = 0.1$) [16, Section 10.5].
- A distortion $r_3 = R_3\overline{x}$ of a low-pass version of $\overline{x}$, where $R_3 = Q_3 \circ L_3$. Here L_3 bandlimits by zeroing all but the 83 lowest-frequency coefficients of the Discrete Fourier Transform, and Q_3 induces componentwise distortion via the operator [16, Section 10.6] $\theta_3 = (2/\pi)\arctan(\gamma_3\cdot)$, where $\gamma_3 = 10$ (see Fig. 2).

The solution space is the standard Euclidean space $\mathcal{H} = \mathbb{R}^N$. To formulate the recovery problem as an instance of (2), set $J = \{1\}$, $J_1 = \varnothing$, $K = \{2, 3\}$, and $C_1 = \big\{x \in \mathcal{H} \;\big|\; f_1(x) \leqslant 0\big\}$, where $f_1 = \|D\cdot\| - \gamma_1$. Then the objective is to

$$\text{find } x \in C_1 \text{ such that } R_2x = r_2 \text{ and } R_3x = r_3. \tag{14}$$

Next, let us verify that Assumption 1(i) is satisfied. On the one hand, since R_2 is the projection onto the closed convex set $[-\gamma_2, \gamma_2]^N$, it is firmly nonexpansive, so we set $S_2 = \mathrm{Id}$. On the other hand, R_3 is proxifiable with $S_3 = \gamma_3^{-1}L_3$ [10]. We thus obtain an instance of (7), to which we apply (11) with (13) and $(\forall n \in \mathbb{N})$ $I_n = J \cup K$ and $(\forall i \in I_n)$ $\omega_{i,n} = 1/3$. The recovered signal shown in Fig. 1 effectively incorporates the information from the prior constraint and the nonlinear distortions.

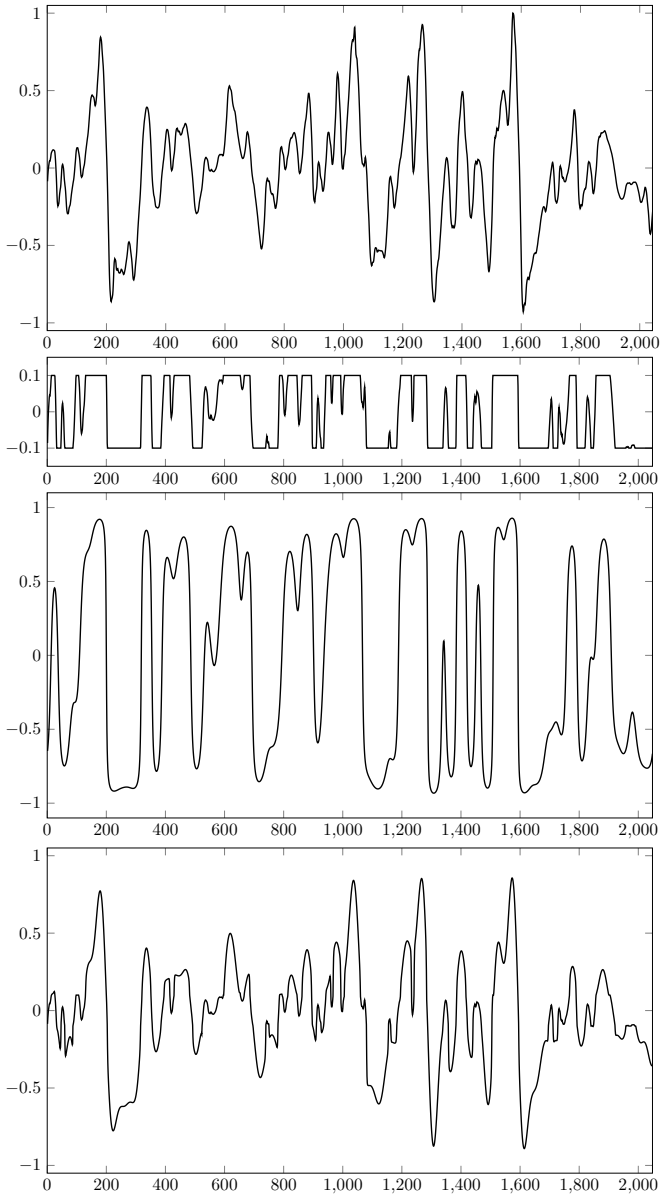

Fig. 1. Signals in Section III-A. Top to bottom: original signal $\overline{x}$, distorted signal r_2, distorted signal r_3, recovered signal.

B. Reconstruction from thresholded scalar products

The goal is to recover the original form of the N-point ($N = 1024$) signal $\overline{x}$ shown in Fig. 3 from thresholded scalar products $(r_k)_{k\in K}$ given by

$$(\forall k \in K) \quad r_k = R_k\overline{x}, \quad \text{with} \quad R_k\colon \mathcal{H} \to \mathbb{R}\colon x \mapsto Q_\gamma\langle x \mid e_k\rangle, \tag{15}$$

where

- $(e_k)_{k\in K}$ is a collection of normalized vectors in $\mathbb{R}^N$ with zero-mean i.i.d. entries.

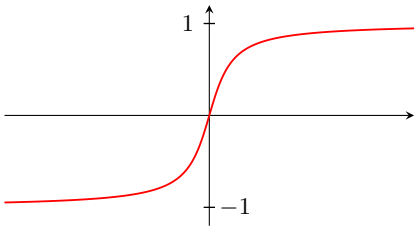

Fig. 2. Distortion operator θ_3 in Section III-A.

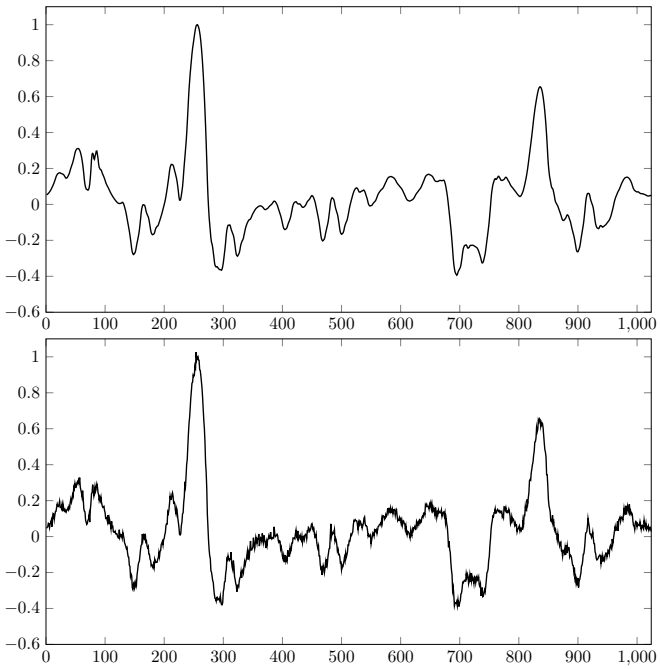

Fig. 3. Original signal $\overline{x}$ (top) and recovery (bottom) in Section III-B.

- Q_γ ($\gamma = 0.05$) is the thresholding operator

$$Q_\gamma \colon \xi \mapsto \begin{cases} \operatorname{sign}(\xi)\sqrt{\xi^2 - \gamma^2}, & \text{if } |\xi| > \gamma; \\ 0, & \text{if } |\xi| \leqslant \gamma \end{cases} \tag{16}$$

  of [15] (see Fig. 4).
- $K = \{1, \ldots, m\}$, where $m = 1200$.

The solution space $\mathcal{H}$ is the standard Euclidean space $\mathbb{R}^N$, and (15) gives rise to the special case of (2)

$$\text{find } x \in \mathcal{H} \text{ such that } (\forall k \in K) \quad r_k = Q_\gamma \langle x \mid e_k \rangle, \tag{17}$$

in which $J = \varnothing$. Note that the standard soft-thresholder on $[-\gamma, \gamma]$ can be written as

$$\operatorname{soft}_\gamma : \xi \mapsto \operatorname{sign}(Q_\gamma \xi) \left(\sqrt{(Q_\gamma \xi)^2 + \gamma^2} - \gamma \right). \tag{18}$$

To formulate (7) we set, for every $k \in K$,

$$S_k \colon \mathbb{R} \to \mathcal{H} \colon \xi \mapsto \operatorname{sign}(\xi) \left(\sqrt{\xi^2 + \gamma^2} - \gamma \right) e_k, \tag{19}$$

which fulfills Assumption 1(i) and yields $S_k \circ R_k = (\operatorname{soft}_\gamma \langle \cdot \mid e_k \rangle) e_k$ [10]. We apply (11) with (13) and the following control scheme. We split K into 12 blocks of 100 consecutive indices, and select I_n by periodically sweeping through the blocks, hence satisfying (12) with $M = 12$. Moreover, $\omega_{i,n} \equiv 1/100$. The reconstructed signal shown in Fig. 3 illustrates the ability of the proposed approach to effectively exploit nonlinearly generated data.

C. Image recovery

The goal is to recover the $N \times N$ ($N = 256$) image $\overline{x}$ from the following (see Fig. 5):

- The Fourier phase $\angle \operatorname{DFT}(\overline{x})$ ($\operatorname{DFT}(\overline{x})$ denotes the 2D Discrete Fourier Transform of $\overline{x}$).
- The pixel values of $\overline{x}$ reside in $[0, 255]$.
- An upper bound γ_3 on the total variation $\operatorname{tv}(\overline{x})$ [8]. In this experiment, $\gamma_3 = 1.2 \operatorname{tv}(\overline{x}) = 1.10 \times 10^6$.
- A compressed representation $r_4 = R_4 \overline{x}$. Here, $R_4 = Q_4 \circ W$, where W is the 2D Haar wavelet transform and Q_4 performs componentwise hard-thresholding via ($\rho = 325$)

$$(\forall \xi \in \mathbb{R}) \quad \operatorname{hard}_\rho \xi = \begin{cases} \xi, & \text{if } |\xi| > \rho; \\ 0, & \text{if } |\xi| \leqslant \rho. \end{cases} \tag{20}$$

- A down-sampled blurred image $r_5 = R_5 \overline{x}$. Here $R_5 = Q_5 \circ H_5$, where the linear operator $H_5 \colon \mathbb{R}^{N \times N} \to \mathbb{R}^{N \times N}$ convolves with a 5×5 Gaussian kernel with variance 1, and $Q_5 \colon \mathbb{R}^{N \times N} \to \mathbb{R}^{8 \times 8}$ maps the average of each of the 64 disjoint 32×32 blocks of an $N \times N$ image to a representative pixel in an 8×8 image [12].

The solution space is $\mathcal{H} = \mathbb{R}^{N \times N}$ equipped with the Frobenius norm $\| \cdot \|$. To cast the recovery task as an instance of (2), we set $J = \{1, 2, 3\}$, $J_1 = \{1, 2\}$, $K = \{4, 5\}$, $C_1 = \{x \in \mathcal{H} \mid \angle \operatorname{DFT}(x) = \angle \operatorname{DFT}(\overline{x})\}$, $C_2 = [0, 255]^{N \times N}$, $f_3 = \operatorname{tv} - \gamma_3$, and $C_3 = \{x \in \mathcal{H} \mid f_3(x) \leqslant 0\}$. Expressions for $\operatorname{proj}_{C_1}$ and ∂f_3 are provided in [11] and [8], respectively. The objective is to

$$\text{find } x \in \bigcap_{j=1}^{3} C_j \text{ such that } \begin{cases} R_4 x = r_4; \\ R_5 x = r_5. \end{cases} \tag{21}$$

Let us verify that Assumption 1(i) holds. For every $\xi \in \mathbb{R}$,

$$\operatorname{soft}_\rho \xi = \operatorname{hard}_\rho \xi + \begin{cases} -\rho, & \text{if } \operatorname{hard}_\rho \xi > \rho; \\ 0, & \text{if } -\rho \leqslant \operatorname{hard}_\rho \xi \leqslant \rho; \\ \rho, & \text{if } \operatorname{hard}_\rho \xi < -\rho. \end{cases} \tag{22}$$

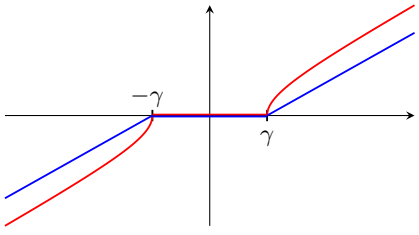

Fig. 4. The thresholder (16) of [15] (red) and the soft thresholder (blue) used in Section III-B.

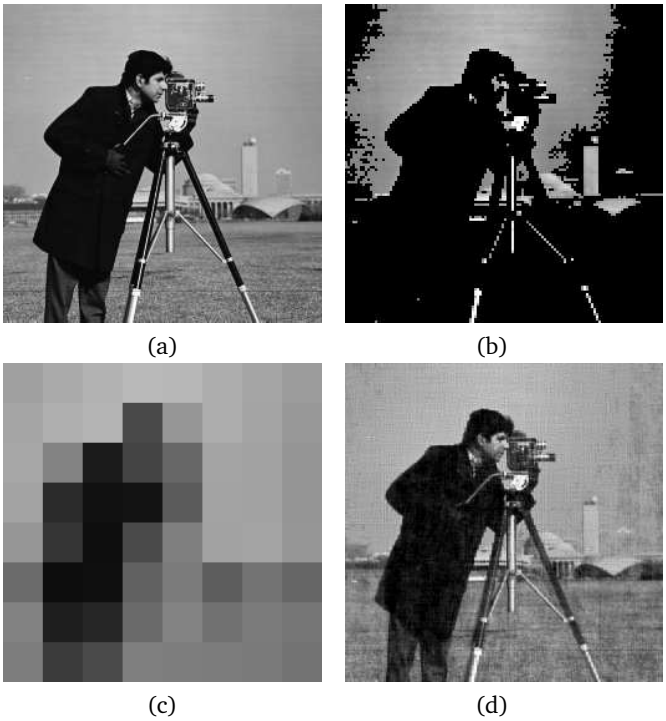

Fig. 5. Images from Section III-C. (a) Original image $\overline{x}$. (b) Compressed image $W^* r_4$. (c) Down-sampled 8×8 image r_5. (d) Recovered image.

We construct S_4 such that $S_4 \circ R_4 = W^{-1} \circ T \circ W$, where T applies soft_ρ componentwise. In turn, recalling that r_4 is the result of hard-thresholding, $S_4 r_4$ is built by first adding the quantity on the right-hand side of (22) to r_4 componentwise, and then applying the inverse Haar transform. This guarantees that S_4 satisfies Assumption 1(i) [10]. Next, we let $D_5 \subset \mathcal{H}$ be the subspace of 32×32-block-constant matrices and construct an operator S_5 satisfying Assumption 1(i) and the identity $S_5 \circ R_5 = H_5 \circ \mathrm{proj}_{D_5} \circ H_5$ [10]. In turn, $S_5 r_5 = H_5 s_5$, where $s_5 \in D_5$ is built by repeating each pixel value of r_5 in the block it represents. We thus arrive at an instance of (7), which we solve using (11) with (13) and

$$(\forall n \in \mathbb{N}) \;\; I_n = J \cup K \text{ and } (\forall i \in I_n)\; \omega_{i,n} = 1/5. \quad (23)$$

The resulting image displayed in Fig. 5(d) shows that our framework makes it possible to exploit the information from the three prior constraints and from the transformations r_4 and r_5 to obtain a quality recovery.

IV. Inconsistent problems

Inaccuracies and unmodeled dynamics may cause (2) to admit no solution. In such instances, we propose the following relaxation for (2) [10].

Assumption 3 For every $j \in J$, the operator proj_{C_j} is easily implementable and, for every $k \in K$, Assumption 1(i) holds. In addition, $\{\omega_j\}_{j\in J} \subset]0,1]$ and $\{\omega_k\}_{k\in K} \subset]0,1]$ satisfy $\sum_{j\in J} \omega_j + \sum_{k\in K} \omega_k = 1$.

Under Assumption 3, the goal is to

$$\text{find} \;\; x \in \mathcal{H} \;\; \text{such that}$$
$$\sum_{j\in J} \omega_j (x - \mathrm{proj}_{C_j} x) + \sum_{k\in K} \omega_k (S_k R_k x - S_k r_k) = 0. \quad (24)$$

When $K = \varnothing$, the solutions of (24) are the minimizers of the least squared-distance proximity function $\sum_{j\in J} \omega_j d^2_{C_j}$ [4]. If (2) does have solutions, then it is equivalent to (24). The algorithm of [7] can be used to solve (24) block-iteratively.

References

[1] H. H. Bauschke and P. L. Combettes, *Convex Analysis and Monotone Operator Theory in Hilbert Spaces,* 2nd ed. New York, NY: Springer, 2017.

[2] T. Blumensath, "Compressed sensing with nonlinear observations and related nonlinear optimization problems," *IEEE Trans. Inform. Theory,* vol. 59, pp. 3466–3474, 2013.

[3] M. Castella, J.-C. Pesquet, and A. Marmin, "Rational optimization for nonlinear reconstruction with approximate ℓ_0 penalization," *IEEE Trans. Signal Process.,* vol. 67, pp. 1407–1417, 2019.

[4] P. L. Combettes, "The Convex Feasibility Problem in Image Recovery," in *Advances in Imaging and Electron Physics,* vol. 95, pp. 155–270. New York, NY: Academic Press, 1996.

[5] P. L. Combettes, "Convex set theoretic image recovery by extrapolated iterations of parallel subgradient projections," *IEEE Trans. Image Process.,* vol. 6, pp. 493–506, 1997.

[6] P. L. Combettes and J. Eckstein, "Asynchronous block-iterative primal-dual decomposition methods for monotone inclusions," *Math. Program.,* vol. B168, pp. 645–672, 2018.

[7] P. L. Combettes and L. E. Glaudin, "Solving composite fixed point problems with block updates," preprint, 2020.

[8] P. L. Combettes and J.-C. Pesquet, "Image restoration subject to a total variation constraint," *IEEE Trans. Image Process.,* vol. 13, pp. 1213–1222, 2004.

[9] P. L. Combettes and N. N. Reyes, "Functions with prescribed best linear approximations," *J. Approx. Theory,* vol. 162, pp. 1095–1116, 2010.

[10] P. L. Combettes and Z. C. Woodstock, "Reconstruction of functions from prescribed proximal points," preprint, 2020.

[11] A. Levi and H. Stark, "Signal reconstruction from phase by projection onto convex sets," *J. Opt. Soc. Amer.,* vol. 73, pp. 810–822, 1983.

[12] K. Nasrollahi and T. B. Moeslund, "Super-resolution: a comprehensive survey," *Mach. Vis. Appl.,* vol. 25, pp. 1423–1468, 2014.

[13] N. N. Reyes and L. J. D. Vallejo, "Global growth of band-limited local approximations," *J. Math. Anal. Appl.,* vol. 400, pp. 418–424, 2013.

[14] D. Rzepka, M. Miśkowicz, D. Kościelnik, and N. T. Thao, "Reconstruction of signals from level-crossing samples using implicit information," *IEEE Access,* vol. 6, pp. 35001–35011, 2018.

[15] T. Tao and B. Vidakovic, "Almost everywhere behavior of general wavelet shrinkage operators," *Appl. Comput. Harmon. Anal.,* vol. 9, pp. 72–82, 2000.

[16] E. Tarr, *Hack Audio: An Introduction to Computer Programming and Digital Signal Processing in MATLAB.* New York, NY: Routledge, 2018.

[17] M. Tofighi, O. Yorulmaz, K. Köse, D. C. Yıldırım, R. Çetin-Atalay, and A. E. Çetin, "Phase and TV based convex sets for blind deconvolution of microscopic images," *IEEE J. Selected Topics Signal Process.,* vol. 10, pp. 81–91, 2016.

[18] H. J. Trussell and M. R. Civanlar, "The feasible solution in signal restoration," *IEEE Trans. Acoustics, Speech, Signal Process.,* vol. 32, pp. 201–212, 1984.

[19] D. C. Youla, "Generalized image restoration by the method of alternating orthogonal projections," *IEEE Trans. Circuits Syst.,* vol. 25, pp. 694–702, 1978.

[20] D. C. Youla and H. Webb, "Image restoration by the method of convex projections: Part 1 – theory," *IEEE Trans. Med. Imaging,* vol. 1, pp. 81–94, 1982.